

Morphology-dependent resonant laser emission of dye-doped ellipsoidal microcavity

Saulius Juodkazis^{a)}

*Satellite Venture Business Laboratory of Photonic Nano-Materials, The University of Tokushima,
2-1 Minamijyosanjima, Tokushima 770-8506, Japan*

Kunihiko Fujiwara, Toshimasa Takahashi, Shigeki Matsuo, and Hiroaki Misawa^{b)}

*Department of Ecosystem Engineering, Graduate School of Engineering, The University of Tokushima,
2-1 Minamijyosanjima, Tokushima 770-8506, Japan*

(Received 14 July 2000; accepted for publication 16 October 2001)

We report a morphology-dependent resonance (MDR) laser emission of rhodamine-doped ellipsoidal microcavity of the poly(methylmethacrylate) particles. Elliptical particles showed different lasing properties: the lasing threshold, intramode spectral separation, mode intensity, and spectral position, when an excitation is pointed to the different locations on the particle. This differs from the well-understood MDR lasing in spherical microparticles. © 2002 American Institute of Physics. [DOI: 10.1063/1.1426240]

I. INTRODUCTION

It is well known that the presence of an optical cavity can significantly change the radiative behavior of an atom or any optical gain medium placed in it. This was predicted by Purcell¹ back in 1946. The more recent concept of photonic crystals^{2,3} can be considered another example of how seemingly inherent properties of spontaneous emission can be engineered. The fluorescence, for example, may be alternatively enhanced or inhibited, depending on whether the emission spectrally coincides with a cavity resonance or photonic bandgap. A cavity enhancement factor F for a three-dimensional cavity of the volume V was derived by Purcell as the following:¹ $F = 3Q\lambda^3/(4\pi^2V)$, where λ is the wavelength and Q is the smallest of the two, the cavity quality $Q = \omega/\Delta\omega$ and the “quality” of the material $Q = \lambda/\Delta\lambda$ are defined by its linewidth $\Delta\lambda$. Factor F represents the ratio of the density of photonic states in the cavity and in the material; in addition, it depends on the refractive index of the material. This dependence can be expressed by an additional factor of $1/n^3$, which means that the Einstein coefficient A depends on both the cavity quality and the volume. A considerable increment of emission is expected for high Q and a small cavity, $V \approx \lambda^3$, which is a technical challenge for fabrication. An experimental observation of Purcell’s effect in the optical spectral range was reported only recently.⁴

Most studies of high- Q lasing modes, referred to as morphology-dependent resonance (MDR), also known as whispering gallery mode, in ring cavity resonators are performed in a microsphere (microdroplet)⁵ or cylinder (fiber)⁶ due to the ease of fabrication and the availability of theoretical simulation. Certain studies have dealt with a deformed sphere cavity with a magnitude of deformation less than 1%.⁷ The MDR models⁵ of a spherical or cylindrical cavity

can be treated analytically, and the effect of small deformations can be included by perturbation theory. However, MDR modes in a further deformed cavity are not perturbatively related to those in the ideal spherical cavities. It is therefore unclear whether high- Q MDR properties still exist in such structures. Theoretically, it was demonstrated that Q spoiling leads to directional radiation output.^{8,9} Recently, the algorithm to calculate the spontaneous emission rate in a microcavity of arbitrary shape was reported, though the calculations were performed only for a microdisk.^{10,11} A significantly deformed sphere, for example an ellipsoid, is promising for utilization as a room-temperature (RT) microparticle-based laser source for photon tunneling applications,¹² a near-field light source, or persistent spectral hole burning memory¹³ where the spectral position of the hole is related to the physical location on the ellipsoidal cavity. Here, we report a MDR laser emission of a rhodamine-doped ellipsoidal microparticle of poly(methylmethacrylate) (PMMA) with an axis ratio of ~ 1.5 . The laser emission was observed in water and air, and it exhibits a significant spectral and polarization dependence on the polarization of excitation.

II. EXPERIMENT

The basic fabrication process of ellipsoidal particles was as follows: first, fixing the dye-doped dielectric polymer spheres into the host polymer cast films at a temperature higher than that for glassy phase transition of the polymer; second, the inlaid spheres were elongated into ellipsoids by pulling the film.

A. Preparation of the elliptical dye-doped PMMA particles

The dye doping of PMMA particles (Sekisui Plastics, MB-50) was carried out as follows: PMMA spheres were dispersed into the methanol solution of rhodamine and kept for 24 h. Two kinds of rhodamine were used, with a photo-

^{a)}Electronic mail: saulius@svbl.tokushima-u.ac.jp

^{b)}Author to whom correspondence should be addressed; electronic mail: misawa@eco.tokushima-u.ac.jp

luminescence maximum at 590 nm (Rh6G from Aldrich Chem.) and 610 nm (RhB from Exiton), respectively, and the type is specified in the text where it applies. The particles were filtered through a 8- μm -pore-diameter filter (Advantec), washed with distilled water, and naturally dried at RT for 24 h. The concentration of rhodamine inside the particles was calculated in the following manner. The rhodamine (RhB or Rh6G) methanol solution of known concentration was prepared for the PMMA soaking of the microparticles. After the dye had permeated the microparticles, the change in the rhodamine concentration was measured and attributed to the amount of dye, which was inside the microparticles. The rhodamine did not leak into the water solution during the procedures of sample preparation (Sec. II B) or during laser manipulation in water (Sec. II C) due to the hydrophobicity of PMMA. The particles fixing was performed by uniform distribution of RhB-doped PMMA spheres into an aqueous solution (10 wt %) of polyvinylalcohol [(PVA), Nacalai-tesque, with degree of polymerization 500]. 5 ml of the mixture was poured onto a slide glass (Matasunami; $26 \times 76 \text{ mm}^2$) and spread over it, then left to dry at RT for several days.

B. Stretching of film and recovery of ellipsoidal PMMA particles

The prolongation of particles was carried out by pulling the formed PVA films with embedded dye-doped PMMA spheres at 120°C – 140°C in an oil bath (Toray Daw Corning Silicone, SRX 390) using a self-made pulling machine. The temperature of the oil was controlled above the glassy phase transition temperature of both PMMA (105°C) and PVA (85°C), and below the melting temperature of rhodamine, which is $\sim 260^\circ\text{C}$. The next step was the separation of the doped-PMMA particles from the PVA film. Because PVA is water soluble and PMMA is not, the prolonged particles were separated by desolving of the film in water. First, the oil adhered around the film was washed off by using hexane, then the film was put into a 80°C isopropanol-water solution (volume ratio 1:9), which was stirred slowly for 15 min. The PVA film was fully resolved, and doped-PMMA particles were left for one day to settle. Then the particles were washed in distilled water and dried, and after drying they looked as presented in Fig. 1. The axis ratio (ratio of the length of major and minor axes) was determined by the degree to which the film was elongated. For example, a pulling from 50 to 70 mm of the film gives an axis ratio of ~ 1.4 in the PMMA particles. Notably, we could not obtain elliptically shaped particles by pulling the film with the inlaid microparticles first, then make a doping; when this was attempted, the PMMA particles were restored to a spherical shape due to the surface tension.

C. Setup for the particle manipulation and measurements

For the measurement of laser emission, the particles were either (i) dispersed in water and manipulated by a continuous wave Nd:YAG laser operating at 1064 nm wavelength, or (ii) spread over the cover glass and illuminated at

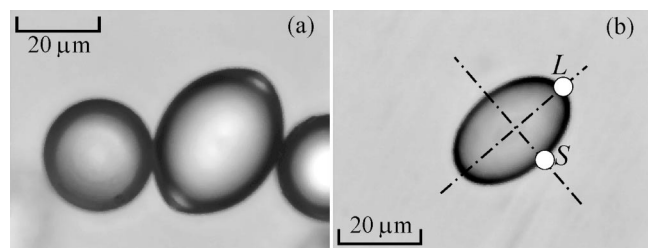


FIG. 1. Microscopic transmission images of PMMA spherical and ellipsoidal microparticles doped with RhB dye. (b) points *L* and *S* are marked on the major (large) and minor (small) axis of the ellipse. These points correspond to the excitation/emission locations used in the experiments.

air ambience without the use of laser manipulation.¹⁴ A 532 nm radiation of *Q*-switched mode-locked Nd:YAG laser (Ekspla, PL-2143A) with a pulse duration of full width at half maximum (FWHM) 30 ps was used for the excitation of emission. In the case of particles dispersed in water, both laser beams were focused by a microscope (Optiphot-2, Nikon) with an objective lens of $40\times$ magnification and with a numerical aperture of $\text{NA}=0.85$. The area of excitation was decided by the size of the focused laser spot, the minimum size of which can be evaluated as $1.22\lambda/\text{NA}=0.76 \mu\text{m}$, where λ is the wavelength of excitation. For the measurements, we used $2 \mu\text{m}$ diameter illumination spots. The detection region was confined by a diameter-adjustable pinhole, from which local light-emitting properties of microparticles were measured, and the pinhole was typically 4–6 μm in diameter. Lasing emission of the microparticles was recorded with a spectrometer (Oriel Instr., Multispec 257) equipped with intensified charge coupled device (CCD) (Hamamatsu Photonics, C4334-01) and having a spectral resolution of 0.05 nm (2400 lines/mm grating). The setup shown in Fig. 2 allowed us to establish and manipulate independently two laser traps. This also allowed us to excite lasing of the one laser-trapped particle and then to approach it to the other in photon tunneling experiments.

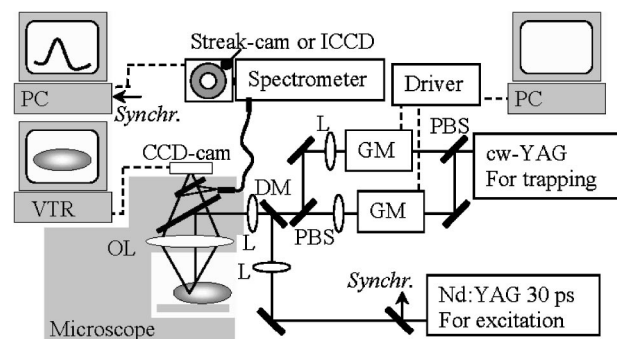


FIG. 2. Experimental setup. Here, OL is the objective lens, L—lens, DM—dichroic mirror, GM—galvano-mirror, PBS—polarized beam splitter, VTR—video tape recorder, and ICCD—intensified charge coupled device. Pulsed Nd:YAG laser was synchronized with a spectral acquisition (marked as *Synchr.*).

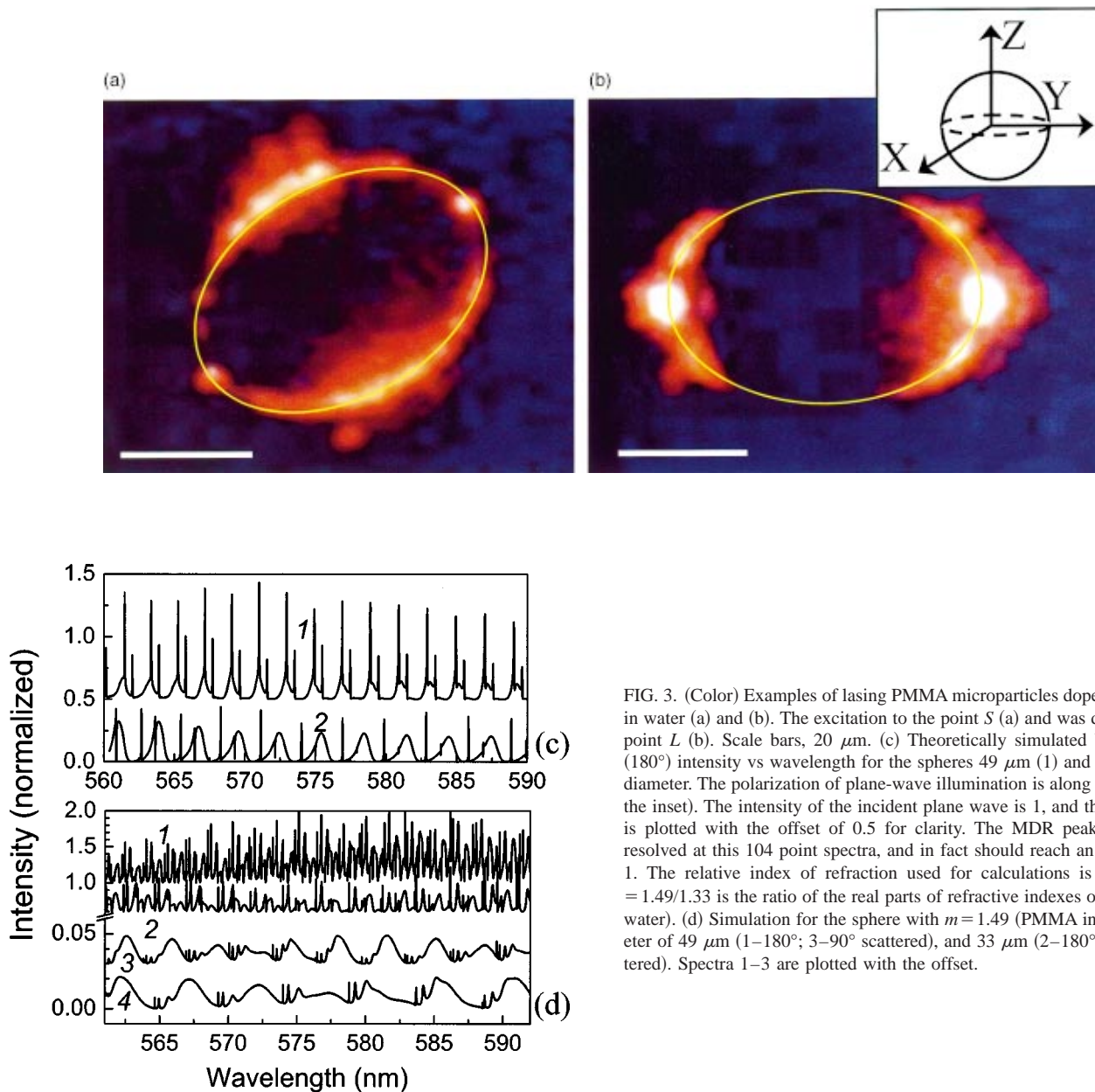


FIG. 3. (Color) Examples of lasing PMMA microparticles doped with Rh6G in water (a) and (b). The excitation to the point *S* (a) and was directly to the point *L* (b). Scale bars, 20 μm . (c) Theoretically simulated backscattered (180°) intensity vs wavelength for the spheres 49 μm (1) and 33 μm (2) in diameter. The polarization of plane-wave illumination is along the *X* axis (in the inset). The intensity of the incident plane wave is 1, and the spectrum *I* is plotted with the offset of 0.5 for clarity. The MDR peaks are not all resolved at this 104 point spectra, and in fact should reach an amplitude of 1. The relative index of refraction used for calculations is $m=1.12$ ($m=1.49/1.33$ is the ratio of the real parts of refractive indexes of PMMA and water). (d) Simulation for the sphere with $m=1.49$ (PMMA in air), a diameter of 49 μm (1– 180° ; 3– 90° scattered), and 33 μm (2– 180° ; 4– 90° scattered). Spectra 1–3 are plotted with the offset.

III. RESULTS AND DISCUSSION

The MDRs are characterized by four parameters: the polarization transverse electric (TE) (without a radial component in the electric field) or transverse magnetic (TM) (without a radial component in the magnetic field), the total angular momentum l , the azimuthal quantum number m , and the radial quantum number n . In a perfect sphere, $2n+1$ azimuthal modes are frequency degenerative, while for an ellipsoid they will be split. The Q factor of the cavity can be estimated by $Q=\omega/(2\gamma)$, where ω is resonant frequency and γ is the FWHM of the lifetime of the lasing line. The Q factor is expected to be lower in the case of elliptical cavity as compared with the spherical one, because the azimuthal modes are not frequency degenerative.

Standing waves result from the total internal reflection at the liquid or air boundary of counter-propagating waves

close to the circumference of the sphere (or ellipse). Laser emission is expected when the round-trip gain is larger than the round-trip loss resulting from optical absorption and radiation leakage (evanescent and refractive). Because the fluorescence linewidth of rhodamine is homogeneously broadened, the emitted radiation will strongly favor those MDRs wavelengths that are within an envelope of dye emission. The characteristic ring-like emission region at the rim of ellipsoids (Fig. 3) suggests the lasing arises from MDRs in the particles. The lasing at the rim of microparticles was observed at whatever point *L* or *S* was illuminated by $\sim 2 \mu\text{m}$ spot at an excitation wavelength of 532 nm [Figs. 3(a) and 3(b)]. The images depict the evanescent and refractive light escape, and the latter is expected to occur more efficiently at the high curvature locations, though not only at those locations.¹⁵

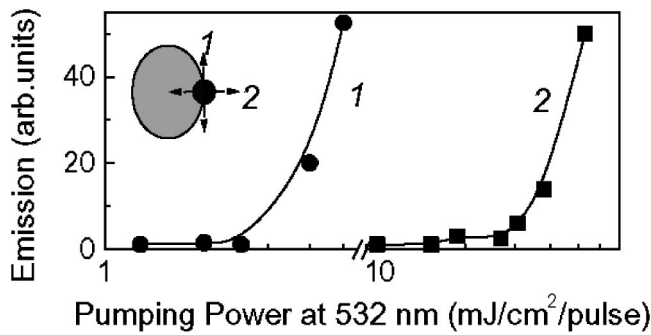


FIG. 4. The dependencies of lasing emission intensity on the illumination power at 532 nm. The polarizations of excitation for the MDR lasing mode at 600.3 nm (1) and 598.8 nm (2), respectively, are shown in the inset. Illumination was directed to and detection was collected from the same point, which is indicated by a black circle [the point S in the notation of Fig. 1(a)]. The PMMA microparticle was doped with RhB, and the major-to-minor axis ratio was 40 μm to 30 μm . The lasing particle was in water.

A. Mie scattering by a sphere

To assess theoretically the expected spectrum of lasing microparticles, the simulation was performed using the code developed by Barber and Hill¹⁶ for the light plane-wave scattering by a sphere. The spectrum of the lasing elliptical microparticle would have different spectral line positions as those from spheres. As the first approach, however, let us calculate the MDR spectra from spherical particles with diameters equal to the major and the minor axis of the elliptical one. The spectral locations of MDRs are related to the spiking features on the Mie light scattering intensity plotted versus the size parameter, $x = 2\pi a/\lambda$, with a being the radius of the sphere. Two spectra presented in Fig. 3(c) were calculated for the backscattered light (as it was actually measured

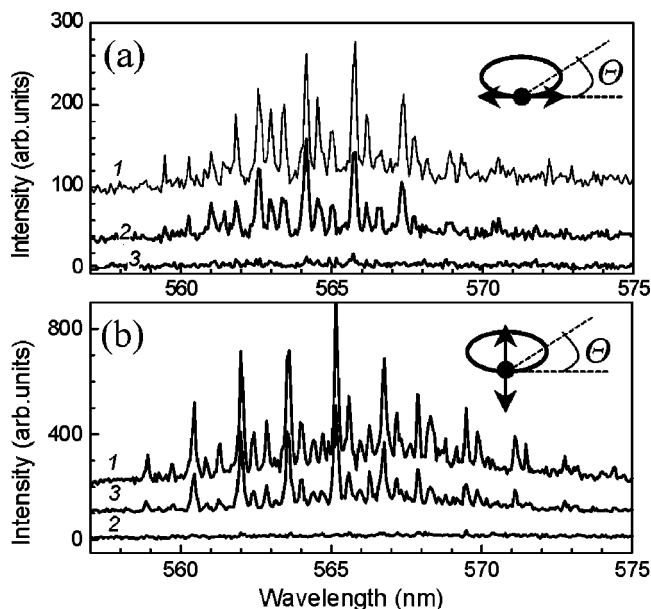


FIG. 5. Polarization dependence of the lasing emission on the polarization of excitation at 532 nm for the point S (excitation and detection at S). The polarization of excitation is indicated by an arrow in the insets, and polarization of the detection was at $\Theta = 0^\circ$ (2); 90° (3); or without an analyzer (1). The PMMA microparticle was doped with Rh6G and the major-to-minor axis ratio was 35 μm to 27 μm . The lasing particle was in air.

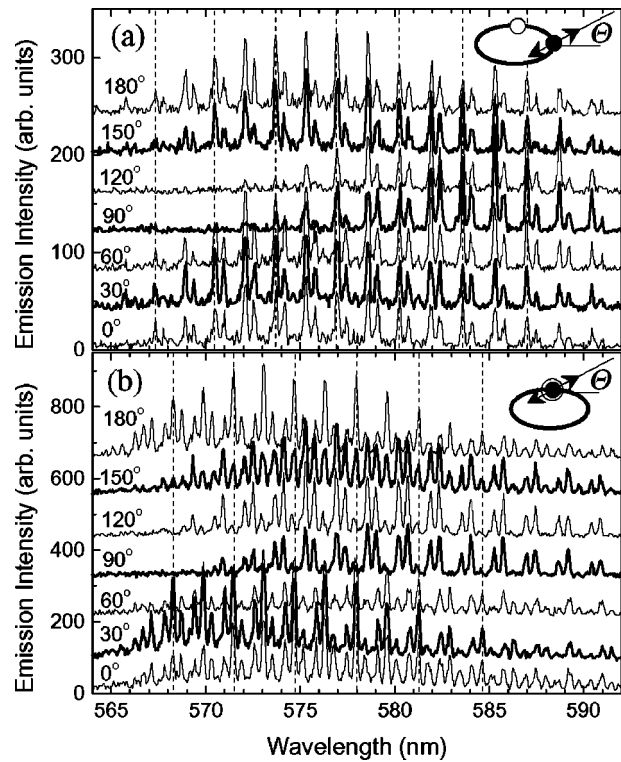


FIG. 6. Dependence of the lasing spectra on the polarization of excitation at 532 nm. (a) excitation (dark circle in the inset) at point L with detection (white circle in the inset) at S. (b) excitation and detection at point S. The angle of polarization is specified at each spectrum. The PMMA microparticle was doped with Rh6G (10^{-2} M concentration) and the major-to-minor axis ratio was 49 μm to 33 μm . Detection was without discrimination in polarization. The lasing particle was in air.

in experiments of lasing microparticles) with a relative refractive index of sphere $m = 1.12$, and the diameters of the spheres were taken to be equal to the length of a major and a minor axis of elliptical particles. The MDRs peaks become narrower as the size parameter increases, and the oscillations are more pronounced for loss-less nonabsorbing spheres (e.g., the MDR spectra become unresolved for the $m = 1.49$, under the same conditions of simulation). In addition, the spectra of MDR (in general, the scattering efficiency and intensity versus size parameter x) are dependent on the observation angle. This feature, caused by the angular dependence of the Legendre, functions for a given size parameter x . It can be seen that the right angle scattered spectrum has periodically missing resonances [curve 4 versus 3 in Fig. 3(d)]. Further, a lasing mode separation in the case of PMMA microparticles in the air is expected to be much smaller than that of microparticles in the water.

B. Spectra of a lasing microparticle

The lasing threshold observed experimentally (Fig. 4) proves the lasing emission. A strong discrimination in the lasing threshold was found (more than tenfold) for two perpendicular polarizations of excitation. This finding can be explained by the lower waveguiding threshold for the TE mode as compared with that of TM,¹⁷ when the “shorter” cavity lasing is excited (along the minor axis of the particle). The emission spectrum at the central part of the particle

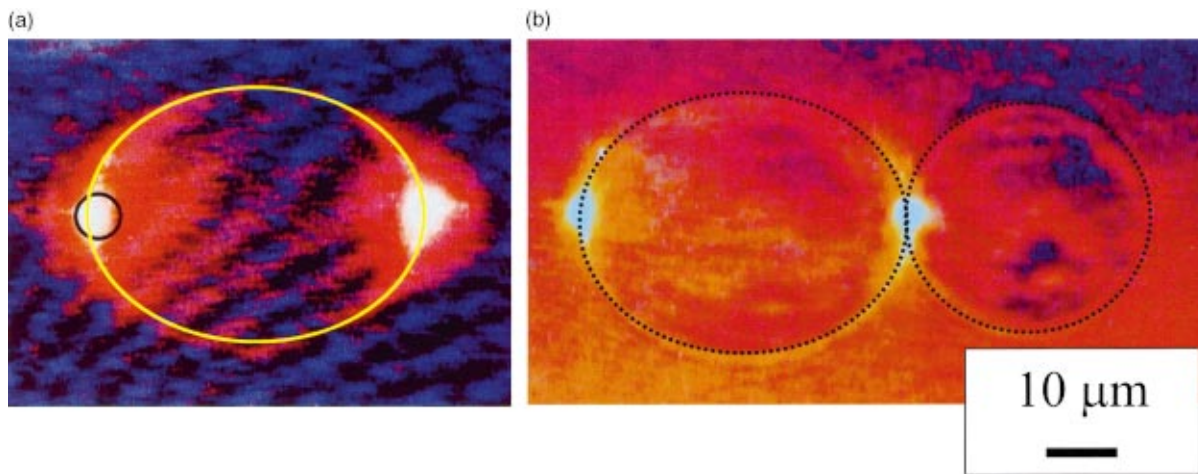


FIG. 7. (Color) Photon tunneling. The intensity of evanescent light (a) was reduced after the lasing particle was approached to the not lasing one (b), which was trapped by a separate laser trap. The PMMA microparticles were laser manipulated in water. The circle in (a) indicates the excitation spot.

gives a very broad featureless band of rhodamine emission. In contrast, the emission spectrum at the particle–air/water boundary shows that the periodically spaced peaks appear over almost the entire fluorescence emission band of RhB or Rh6G (when the corresponding dye was used). This result suggests that the lasing is based on MDRs, and laser emission leaks by refraction from the particle along its rim (Fig. 5). The high Q -factor value was estimated for a MDR lasing $Q = \lambda/\Delta\lambda \approx 4710$ for the highest intensity peak in Fig. 5 (curve 1). It can be seen that the polarization of the registered emission is preferentially polarized along the polarization of excitation, as could be expected. The mode spacing for spherical particles, $\Delta\lambda$, can be calculated from the Mie scattering theory^{18,19} as

$$\Delta\lambda_{\text{sphere}} = \frac{\lambda^2}{2\pi a n_2} \frac{\sqrt{\tan^{-1}(n_1/n_2)^2 - 1}}{\sqrt{(n_1/n_2)^2 - 1}}, \quad (1)$$

where $n_1 = 1.49$ and n_2 are the refractive indexes of PMMA and the ambient of the particle (water or air, with their corresponding refractive indices of 1.33 or 1) at $\lambda \approx 600$ nm, respectively.²⁰ Experimental observations closely follow this equation as we reported earlier in the case of dye-doped PMMA microparticles.¹⁹

This gives the theoretical estimate for a lasing sphere in air; $\Delta\lambda$ (33- μm -diameter) = 1.44 nm and $\Delta\lambda$ (49- μm -diameter) = 0.97 nm (these are the diameters of the major and minor axes of the particle, respectively, for which the lasing is presented in Fig. 6).

Experimentally, the same spectral separation of the most pronounced lasing peaks was found at 1.63 ± 0.05 nm for microparticles in air (Fig. 6), independent of which excitation point L or S was used (the measurement of emission was carried out at the same point ' S '). Meanwhile, the modal substructure of the lasing spectrum appeared different for the excitations at points S or L , and was dependent on the polarization of excitation [Figs. 6(a) versus 6(b)]. If compared with the theoretical evaluation by Eq. (1), it is evident that the most intense modes correspond to the shorter cavity. The substructure of less spectrally separated modes can also be

resolved, as shown in Figs. 5 and 6. Only the intensity of the same spectral modes was observed changing along with the change of excitation polarization (Fig. 6). The polarization dependence of the lasing threshold and spectrum suggests the excitation of TE and TM guiding modes inside a cavity of the microparticle. A complex modal structure of lasing radiation and its polarization dependence is most probably related to the recently reported polarization conversion and interference of the copropagating and counterpropagating modes in the microcavity.²¹ The envelope of the spectrum was shifted by 5–7 nm when the polarization of excitation was changed from $\Theta = 0^\circ$ to 90° , and this change was of the order of 0.5 in terms of the FWHM of all spectral envelope of the microparticle emission. This is a feature, related specifically to the elliptical shape of the particle, given that no such dependence was observed in the emission of spherical particles,^{22,23} in which all lasing modes come out of the cavity with the same length. A possible application of this feature could be the polarization- or location- (location of excitation on the microparticle) dependent spectral hole burning memory. In other words, the polarization or location of the irradiation spot could be “remembered” by a single microparticle once the lasing can induce the spectral hole burning (transient or persistent) in the particle. This phenomenon has already been demonstrated in an ensemble of spherical microparticles of different diameters.¹³ Other applications, similar to the reported microdisk-waveguide coupler²⁴ may be realized on the basis of the polarization-dependent lasing of microparticles. Polarization control over an optical switching could be made possible.

An additional possible application of the elliptical cavity lies in the field of point-light sources. The elliptical cavity has the advantage here over the spherical cavity,²⁵ due to the expected directional output of the former.¹⁵ Experimentally, we observed a decrease of the light intensity when the lasing elliptical microparticle was approached to the other particle down to the distance ($< \lambda/10$), which is sufficient for photon tunneling (Fig. 7). The dye-doped liquid pendant droplets can also be shaped into an elliptical or quadruple-like cavity

by the applied external electrical field, as demonstrated recently.²⁶ However, the polymer-based lasing microparticles are more practical point-like light sources, because the pendant droplets are usually changing their shape while lasing by evaporation, and, consequently, their lasing properties are simultaneously changing.

IV. CONCLUSIONS

The lasing out of the PMMA—rhodamine elliptical microparticle cavity has been demonstrated. The lasing was observed in both water and air when the inside rhodamine concentration was 10^{-3} – 10^{-2} M. The lasing exhibited different lasing thresholds in response to the different excitation polarizations. Spectral mode separation was similar to that in spherical microparticles. We observed the spectral dependence of the output emission on the polarization of excitation. Photon tunneling is demonstrated by laser manipulation of the lasing microparticle.

ACKNOWLEDGMENTS

The present work was partly supported by the Satellite Venture Business Laboratory of the University of Tokushima.

¹E. M. Purcell, *Phys. Rev.* **69**, 681 (1946).

²E. Yablonovitch, *Phys. Rev. Lett.* **58**, 2059 (1987).

³S. John, *Phys. Rev. Lett.* **58**, 2486 (1987).

⁴J. M. Gerard, B. Sermage, B. Gayral, B. Legrand, E. Costard, and V. Thierry-Mieg, *Phys. Rev. Lett.* **81**, 1110 (1998).

⁵R. E. Benner, P. W. Barber, J. F. Owen, and R. K. Chang, *Phys. Rev. Lett.* **44**, 475 (1980).

⁶J. F. Owen, P. W. Barber, P. B. Dorain, and R. K. Chang, *Phys. Rev. Lett.* **47**, 1075 (1981).

⁷J. C. Swindal, D. H. Leach, R. K. Chang, and K. Young, *Opt. Lett.* **18**, 191 (1993).

⁸J. U. Nöckel, A. D. Stone, and R. K. Chang, *Opt. Lett.* **19**, 1693 (1994).

⁹A. Mekis, J. U. Nöckel, G. Chen, A. D. Stone, and R. K. Chang, *Phys. Rev. Lett.* **75**, 2682 (1995).

¹⁰Y. Xu, R. K. Lee, and A. Yariv, *Phys. Rev. A* **61**, 033808 (2000).

¹¹Y. Xu, R. K. Lee, and A. Yariv, *Phys. Rev. A* **61**, 033807 (2000).

¹²K. Sasaki, H. Misawa, N. Kitamura, R. Fujisawa, and H. Masuhara, *Jpn. J. Appl. Phys., Part 2* **32**, L1144 (1993).

¹³S. Arnold, C. Liu, W. B. Whitten, and J. M. Ramsey, *Opt. Lett.* **16**, 420 (1991).

¹⁴K. Kamada, K. Sasaki, R. Fujisawa, and H. Misawa, in *Microchemistry*, edited by H. Masuhara (Elsevier, Amsterdam, 1994), pp. 287–300.

¹⁵C. Gmachl, F. Capasso, E. E. Narimov, J. U. Nöckel, A. D. Stone, J. Faist, D. L. Sivco, and A. Y. Cho, *Science* **280**, 1556 (1998).

¹⁶P. W. Barber and S. C. Hill, *Light Scattering by Particles: Computational Methods* (World Scientific, Singapore, 1990).

¹⁷H. Nishihara, M. Haruna, and T. Suhara, *Optical Integrated Circuit* (McGraw-Hill, New York, 1989), Chap. 8, pp. 224–244.

¹⁸J. L. Cheung, J. M. Hartings, and R. K. Chang, in *Handbook of Optical Properties: Optics of Small Particles, Interfaces, and Surfaces*, edited by R. E. Hummel and P. Wissmann (CRC Press, Boca Raton, 1997), pp. 233–260.

¹⁹T. Takahashi, K. Fujiwara, S. Matsuo, and H. Misawa, *J. Photochem. Photobiol., A* **120**, 135 (1999).

²⁰H. Misawa, R. Fujisawa, K. Sasaki, N. Kitamura, and H. Masuhara, *Jpn. J. Appl. Phys., Part 2* **32**, L788 (1993).

²¹M. L. M. Balistreri, D. J. W. Klunder, F. C. Blom, A. Driessen, H. W. J. M. Hoekstra, J. Kortrijk, L. Kuipers, and N. F. van Hulst, *Opt. Lett.* **24**, 1829 (1999).

²²T. Takahashi, S. Matsuo, H. Misawa, T. Karatsu, A. Kitamura, K. Kamada, and K. Ohta, *Thin Solid Films* **331**, 298 (1998).

²³T. Takahashi, S. Matsuo, H. Misawa, T. Karatsu, A. Kitamura, K. Kamada, and K. Ohta, *Nonlinear Opt.* **22**, 397 (1999).

²⁴F. C. Blom, D. R. van Dijk, H. J. W. M. Hoekstra, A. Driessen, and T. J. A. Popma, *Appl. Phys. Lett.* **71**, 747 (1997).

²⁵H. Fujiwara and K. Sasaki, *J. Appl. Phys.* **86**, 2385 (1999).

²⁶X.-Y. Pu and W.-K. Lee, *Opt. Lett.* **25**, 466 (2000).